Engagement of basal amygdala-nucleus accumbens glutamate neurons in the processing of rewarding or aversive social stimuli

RESEARCH REPORT

Engagement of basal amygdala-nucleus accumbens glutamate neurons in the processing of rewarding or aversive social stimuli

Giulia Poggi[1] | Giorgio Bergamini[1] | Redas Dulinskas[1] | Lorraine Madur[1,2] | Alexandra Greter[1] | Christian Ineichen[1] | Amael Dagostino[1] | Diana Kúkeľová[1] | Hannes Sigrist[1] | Klaus D. Bornemann[3] | Bastian Hengerer[3] | Christopher R. Pryce[1,2] [ID]

[1]Preclinical Laboratory for Translational Research into Affective Disorders, Department of Psychiatry, Psychotherapy and Psychosomatics, Psychiatric University Hospital Zürich (PUK) and University of Zurich (UZH), Zurich, Switzerland

[2]Zurich Neuroscience Center, University of Zurich and Swiss Federal Institute of Technology, Zurich, Zurich, Switzerland

[3]CNS Diseases Research, Boehringer Ingelheim Pharma GmbH & Co. KG, Biberach, Germany

Correspondence
Giulia Poggi and Christopher R. Pryce, Preclinical Laboratory for Translational Research into Affective Disorders, Department of Psychiatry, Psychotherapy and Psychosomatics, Psychiatric University Hospital Zurich (PUK) and University of Zurich (UZH), August Forel-Strasse 7, CH-8008 Zurich, Switzerland.
Email: giulia.poggi@bli.uzh.ch and christopher.pryce@bli.uzh.ch

Funding information
Boehringer-Ingelheim Innocentive grant, Grant/Award Number: 230475; Swiss National Science Foundation, Grant/Award Number: 31003A_179381

Edited by: David Belin

Abstract

Basal amygdala (BA) neurons projecting to nucleus accumbens (NAc) core/shell are primarily glutamatergic and are integral to the circuitry of emotional processing. Several recent mouse studies have addressed whether neurons in this population(s) respond to reward, aversion or both emotional valences. The focus has been on processing of physical emotional stimuli, and here, we extend this to salient social stimuli. In male mice, an iterative study was conducted into engagement of BA-NAc neurons in response to estrous female (social reward, SR) and/or aggressive-dominant male (social aversion, SA). In BL/6J mice, SR and SA activated c-Fos expression in a high and similar number/density of BA-NAc neurons in the anteroposterior intermediate BA (int-BA), whereas activation was predominantly by SA in posterior (post-)BA. In *Fos-TRAP2* mice, compared with SR-SR or SA-SA controls, exposure to successive presentation of SR-SA or SA-SR, followed by assessment of tdTomato reporter and/or c-Fos expression, demonstrated that many int-BA-NAc neurons were activated by only one of SR and SA; these SR/SA monovalent neurons were similar in number and present in both magnocellular and parvocellular int-BA subregions. In freely moving BL/6J mice exposed to SR, bulk GCaMP6 fibre photometry provided confirmatory in vivo evidence for engagement of int-BA-NAc neurons during social and sexual interactions.

Abbreviations: 4-OHT, 4-Hydroxytamoxifen; AO, Aversive odour; BA, Basal amygdala; NAc, Nucleus accumbens; No S, No stimulus; SA, Social aversion; SR, Social reward; TMT, Trimethylthiazoline; TRAP2, Targeted recombination in active populations 2.

Therefore, populations of BA-NAc glutamate neurons are engaged by salient rewarding and aversive social stimuli in a topographic and valence-specific manner; this novel evidence is important to the overall understanding of the roles of this pathway in the circuitry of socio-emotional processing.

1 | INTRODUCTION

Accurate detection of and adaptive responding to emotionally salient stimuli are vital brain functions; this applies to both rewarding stimuli that elicit appetitive and consummatory behaviours and aversive stimuli that elicit defensive avoidance and escape behaviours. Pathologies of emotional stimulus processing constitute major symptoms in various neuropsychiatric disorders, including major depressive disorder, schizophrenia and social anxiety disorder. The amygdala is a major region in the neural circuitries of both aversion and reward processing (Baxter & Murray, 2002; Lüthi & Lüscher, 2014). The lateral amygdala (LA) and basal/basolateral amygdala (BA) are cortex-like, comprising primarily pyramidal glutamatergic neurons (Belova et al., 2007; Duvarci & Pare, 2014; Johansen et al., 2011; Pitkänen et al., 1997). Glutamate neurons in LA receive and integrate inputs from thalamic and cortical sensory neurons encoding innate and conditioned stimuli (Johansen et al., 2011) and are the major afferents onto BA glutamate neurons (Duvarci & Pare, 2014; Pitkänen et al., 1997). The function(s) of BA glutamate neurons is less well understood: they project to several sub-cortical and cortical regions, including nucleus accumbens (NAc) core and shell, which are also major regions of reward and aversion processing (Beyeler et al., 2018; Burgos-Robles et al., 2017; Duvarci & Pare, 2014).

In mice, a small number of studies of amygdala processing of stimulus valence (reward and aversion) have included the amygdala-to-NAc neural pathway. Firstly, in a study of LA/BA-NAc neurons, neuronal density was highest in the anteroposterior (AP) intermediate LA/BA (Beyeler et al., 2018; Namburi et al., 2015), where the BA comprises both medial anterior/magnocellular and lateral posterior/parvocellular subregions (Pitkänen et al., 1997). Using in vivo single-cell electrophysiological recording to measure responsiveness of LA/BA-NAc neurons to reward (sucrose) or aversion (quinine), 16% were excited by sucrose (reward neurons), 3% by quinine (aversion neurons) and 3% by sucrose and quinine (dual-valent neurons; Beyeler et al., 2016, 2018). Second, putative marker genes were used to identify and distinguish

between neurons responsive to reward (female) and aversion (foot shock): 70% of BA-NAc neurons were identified as reward neurons (i.e. expressed the putative reward-neuron gene *Ppp1r1b*) and were posterior/parvocellular, and the remaining 30% were identified as aversion neurons (expressed the putative aversion-neuron gene *Rspo2*) and were intermediate/magnocellular (Kim et al., 2016). Third, putative marker genes were used to identify reward (sucrose) and aversion (air puff and tail shock) neurons: all BA-NAc neurons were identified as aversion neurons (expressed the putative aversion-neuron gene *Fezf2*) and were anterior (Zhang et al., 2021). In addition to the discrepancies in the findings of these studies, another feature of BA-NAc neuron research to date has been the focus on physical emotional stimuli. In male mice, estrous female was applied as a social reward (SR) stimulus in only a single study (Kim et al., 2016), and aggressive-dominant male as social aversion (SA) stimulus remains to be applied.

Given the particularly high emotional salience of social stimuli (Griffin et al., 2002; Kirschbaum et al., 2004; McEwen, 2007) and the common application of aggressive-dominant male as a chronic stressor (Gururajan et al., 2019; Pryce & Fuchs, 2017), a study directly comparing engagement of BA-NAc neurons by estrous-receptive female and aggressive-dominant male would be informative. The iterative aims of the current study were to: (1) establish the AP distribution of retrogradely-labelled BA-NAc (core and shell) neuronal somata activated in terms of c-Fos by SR and/or SA. (2) Using targeted recombination in active populations (TRAP) in an AP subregion with a relatively high density of SR and SA BA-NAc neurons, determine whether they are monovalent or dual-valent. (3) Having identified the engagement of BA-NAc neurons by SR (or SA) using ex vivo methods, apply bulk calcium-sensor fibre photometry to provide in vivo evidence for engagement of BA-NAc neurons during either distal or proximal interactions with SR. Aim 1 demonstrated that AP-intermediate BA was relatively rich in BA-NAc neurons responsive to SR and/or SA, and AP-posterior BA (post-BA) was also rich in BA-NAc neurons responsive to SA. Aim 2 demonstrated that substantial and equable

proportions of intermediate BA-NAc neurons were monovalent with respect to SR and SA. Aim 3 demonstrated that intermediate BA-NAc neurons were engaged during distal and proximal interactions with SR. These findings further the understanding of the anatomical organization and valence specificity of BA-NAc neurons engaged in the processing of social stimuli of high emotional significance. They are relevant to both adaptive socio-emotional processing and the pathologies thereof that are common in stress-related neuropsychiatric disorders.

2 | MATERIAL AND METHODS

2.1 | Animals

Experiments were conducted with male mice of the C57BL/6J (BL/6) strain, and male offspring of Fos-TRAP2$^{+/+}$ sires ($Fos^{tm2.1[icre/ERT2]Luo}$/J; IMSR_JAX:030323) and Ai14$^{+/+}$ dams (B6.Cg-Gt(ROSA) 26Sor$^{tm14(CAG-tdTomato)Hze}$/J; IMSR_JAX:007908) that were therefore of genotype Fos-TRAP2$^{+/-}$ x Ai14$^{+/-}$ and are referred to as strain *Fos-TRAP2* (DeNardo et al., 2019; Madisen et al., 2010). All experimental mice were bred in-house, weaned with same-sex littermates at age 4 weeks, and maintained in littermate pairs from age 5–6 weeks until the end of the experiment, unless stated otherwise below. Mice were maintained in cages measuring 33 × 21 × 14 cm in an individually ventilated caging (IVC) system. Temperature was kept at 21–23°C and humidity at 50%–60%, and the light cycle was reversed with lights off at 7:00 AM–7:00 PM. Mice were fed ad libitum with food pellets (Complete pellet, Provimi, Kliba AG, Kaiseraugst, Switzerland), and water was also provided ad libitum. All experimental procedures were conducted during the dark phase and between 9:00 AM and 5:00 PM. Each experiment began with the handling of each mouse for 5 min per day on each of three to five consecutive days, including control mice that were not exposed to a social stimulus (see below). All experiments were conducted under an animal experiment licence issued by the Veterinary Office of Canton Zurich (ZH-155/2018).

2.2 | Stereotactic surgery for retrograde tracing and fibre photometry

Stereotactic surgery was performed using an Angle Two™ system (Leica) according to our previously published protocol (e.g. Ineichen et al., 2022). Both mice per littermate pair were operated consecutively on the same

day. Analgesia was conducted with buprenorphine and anaesthesia with isoflurane in pure oxygen. Cranial burr holes (Ø = 300 μm) were drilled for bilateral injection of retrograde tracer cholera toxin subunit β (ex vivo assessment of neuronal activation) or unilateral injection of viral vectors and placement of an optic fibre (in vivo GCaMP6 fibre photometry). Injections were conducted at a rate of 50 nL/min using 10 μL NanoFil™ microsyringes fitted with a 33 G bevelled stainless-steel needle and connected to an ultra-micro pump (UMP3, Micro4; World Precision Instruments). After injection completion, the microsyringe remained in position for 5 min and was then slowly withdrawn. Concerning stereotactic injection coordinates, based on a mouse brain atlas (Franklin & Paxinos, 2019), for NAc, these were bregma anterior-posterior (AP) +1.1 or +1.6 mm, medial-lateral (ML) ±1.1 mm, dorsal-ventral (DV) −4.8 mm. Coordinates selection, in particular AP, was informed by previous studies with which we wanted to maximize comparison (Kim et al., 2016; Namburi et al., 2015), and also enabled the targeting of BA projectors to both core and shell NAc subregions. For fibre photometry, coordinates for AAV vector injection in BA were bregma AP −1.8 mm, ML ± 3.2 mm, DV −5.1 mm (Franklin & Paxinos, 2019); these were based on current ex vivo findings and published evidence (Beyeler et al., 2018) that the absolute number of BA neurons projecting to NAc at bregma +1.1 is highest at bregma −1.6 to −2.0. Mice were weighed and wound healing controlled for 10 days post-surgery. Neuronal activation was also studied for BA neurons projecting to the lateral and medial compartments of the central amygdala. For this experiment, cholera toxin subunit β was injected bilaterally using the coordinates AP −0.9 mm, ML ± 2.6 mm, DV −4.9 mm.

2.3 | Establishing distribution profiles of stimulus-responsive BA neurons projecting to NAc

The aims of this experiment were to quantify the AP distribution of BA neuronal cell bodies projecting to NAc and of the responsiveness of these BA-NAc neurons to social stimuli as determined using c-Fos activation.

2.3.1 | Experimental design

BL/6 mice (n = 45) were infused bilaterally in NAc with the retrograde neuronal tracer, recombinant cholera toxin subunit β conjugated with Alexa Fluor™ 555 (CTB-555, Invitrogen); 300 nL of 1 mg/mL were injected per NAc. At 14 days post-surgery, mice were single-caged

and, after a further 3–4 days, assigned at random to the following stimulus groups: SR ($n = 12$), SA ($n = 12$), aversive odour (AO, $n = 7$), and no stimulus (No S, $n = 14$). Directly after completion of the 90-min stimulus test, mice were deeply anaesthetized and transcardially perfused-fixed. The brains were further processed for c-Fos immunohistochemistry and quantification of CTB^+, $c\text{-}Fos^+$ and $CTB^+/c\text{-}Fos^+$ neurons across the AP and ML extents of the BA.

2.3.2 | Stimulus exposure protocols

All protocols were conducted between 9:00 AM and 1:00 PM, that is, in the first half of the dark phase. Table S1 summarizes the conditions used for stimulus pre-exposure and test in this and the other experiments.

SR

At the onset of the dark phase on Days 15 and 16 post-surgery, adult female BL/6 mice were screened for reproductive stage: vaginal lavage was conducted by gently pipetting up and down 50 μL sterile ddH$_2$O at the opening of the vagina. The derived cell suspension was transferred onto a glass slide and placed at 37°C until dry. The cells were then stained with 50 μL 0.1% cresyl violet, cover-slipped and assessed at the microscope (Ekambaram et al., 2017). Females that were at proestrus or oestrus were included as SR stimuli. An unfamiliar (pro-)estrous female was introduced into the home cage of the male for test onset (t_0). Behavioural events were observed during 90 min using an ethogram (Table S2); it was noted whether each of mount, copulate and penis lick occurred. If males showed at least one mount within min 1–20 the protocol was continued; if the female was not receptive, despite being at the appropriate oestrus cycle stage, and repeatedly avoided the male, the protocol was discontinued and the male was presented with another female on the following day. After 90 min (t_{90}), the female was returned to its home cage and the male was processed for brain perfusion-fixation.

SA

The protocol comprised three stages conducted within a period of 6 days in the colony room. In the habituation stage on Days 15–17 post-surgery, the home cage of the male was divided by placing a transparent, perforated plastic divider along its length for 20 min per day. In the pre-exposure stage on Day 18, the same divider was placed in the cage of an aggressive, ex-breeder CD-1 male aged 8–10 months and weighing 38–55 g (Janvier Labs, France). The BL/6 mouse was introduced into the same compartment as the CD-1 mouse and received a cumulative total of 60 s physical attack maximum or at least 30 s physical attack during 10 min maximum (see ethogram, Table S2). The BL/6 mouse was then returned to the home cage and left undisturbed for 24–48 h. This primed the BL/6 male so that distal and proximal exposure to the CD-1 mouse was aversive in the final test stage. In the SA test on Day 20, the same divider was placed in the cage of the same CD-1 mouse: the BL/6 mouse was placed in the opposite compartment to the CD-1 mouse for test onset (t_0) and exposed to distal aversion (visual, olfactory and auditory) for 20 min; it was then placed in the same compartment as the CD-1 mouse (proximal) for 30–60 s cumulative physical attack during 10 min maximum, and then remained in this compartment whilst the CD-1 mouse was transferred to the other compartment (distal aversion) until t_{90} (Table S2). The BL/6 mouse was then returned to its home cage and processed for brain perfusion-fixation.

AO

As a physical aversive stimulus, 2,5-dihydro-2,4,5-trimethylthiazoline (TMT, 1 g/mL; Angene International, Hong Kong), a constituent of fox urine/faeces with an odour innately aversive to rodents (Rosen et al., 2015), was used. The BL/6 mice were transferred to a remote and isolated room on Days 15 and 16 post-surgery and allowed to acclimatize. On Day 17, a paper tissue was inserted into a 50 mL Falcon tube and 500 μL TMT were pipetted onto the tissue, and the tube without cap was placed on top of the grid of the home cage and covered with the cage lid (t_0). The mouse could not physically contact the tissue but the TMT odour permeated the cage. The following behaviours occurred and were maintained throughout the majority of the protocol: piloerection, inactivity, huddling in a corner or in the sleeping house. At t_{90}, the mouse was processed for brain perfusion-fixation.

No S

To provide a comparison group of basal c-Fos activity in BA-NAc neurons, No S mice remained undisturbed in the colony room in their home cage until being processed for brain perfusion-fixation. On each day that stimulus exposure was run, one to three No S mice were also included in the experiment. One limitation of the experiment is that SA mice were transferred to a familiar cage whereas SR and No S mice remained in their home cage. In future studies, it would be advantageous to include an additional control group in which brain collection follows transfer to a familiar cage containing the type of divider used for SA.

2.3.3 | Immunohistochemistry and confocal microscopy

Mice were deeply anaesthetized with pentobarbital (150 mg/kg intraperitoneal [i.p.]) followed by transcardial perfusion-fixation with phosphate-buffered saline (PBS, pH 7.4, 20 mL) and then freshly-prepared ice-cold paraformaldehyde (PFA, 4% in 0.4 M sodium phosphate buffer, 50 mL). Brains were extracted and placed in 4% PFA for post-fixation for 5 h, and transferred into 30% sucrose solution for 48 h, before embedding in cryoprotective medium (Tissue-TEK OCT Compound), freezing on powdered dry ice and storing at −80°C. Using a cryostat (Leica) at −18°C, brains were sectioned coronally at 40 μm. A mouse brain atlas (Franklin & Paxinos, 2019) was used to identify sections at the appropriate bregma levels. For c-Fos immunofluorescence, five series of sections including BA were collected from −1.0 to −2.6 mm, one section per 200 μm per series. The sections were stored in cryoprotective solution (glycerine and ethylene glycol in 0.2 M phosphate buffer; Sigma-Aldrich) at −20°C until further processing. For c-Fos immunofluorescence, sections were transferred to a 24-well plate (two sections/well) and washed 3 × 20 s in Tris-Triton buffer (pH 7.4) on a shaker. Sections were blocked in 2% goat or donkey serum (Sigma-Aldrich) in 0.2% Triton X-100 in Tris-Triton for 60 min at RT on a shaker, and incubated with 1:1000 rabbit anti-c-Fos 9F6 (Cell Signaling Technology Cat# 2250, RRID:AB_2247211) in blocking solution for 18 h at 4°C on a shaker. Sections were washed in Tris-Triton for 3 × 20 s at RT and incubated with secondary antibody in blocking solution for 120 min at RT on a shaker: depending on the CTB conjugated fluorophore, either 1:500 goat anti-rabbit cyanine5 (A10523, Thermo-Fisher Scientific, RRID:AB_2534032) or 1:500 donkey anti-rabbit Alexa Fluor 488 (A-21206, ThermoFisher Scientific, RRID:AB_2535792). The sections were washed 3 × 20 s in Tris-Triton, transferred to 1× PBS, and mounted on microscope slides (SuperFrost, Epredia). Fluoroshield with DAPI (F6057, Sigma-Aldrich) was added, and the sections cover-slipped for microscopy.

Section images were acquired using an inverted confocal laser scanning microscope (Leica SP8) fitted with an HC PL APO CS2 20× NA 0.75 multi-immersion objective in standard mode. The pinhole was set to 1 AU (airy units), pixel size to $1.14 \times 1.14 \ \mu m^2$, and z-stack step size to 2 μm. Following the acquisition of the z-stack images, the area of interest per hemisphere was defined, and these were analysed using a macro custom-written in Fiji (Schindelin et al., 2012) for identification and quantification of CTB, c-Fos and DAPI, with the experimenter blinded with respect to mouse ID and group. Areas that were CTB^+ or $c\text{-}Fos^+$ were automatically filtered for size, with the range 10–300 pixels used to define cell bodies. CTB^+ or $c\text{-}Fos^+$ areas were also automatically filtered with respect to the threshold for the grey value that differentiated signal from background: this was established empirically for each marker; for CTB one threshold was used for all images of each mouse and adjusted mildly between mice, and for c-Fos one threshold was used across all images. Visual inspection of the binary mask output confirmed that automated counting yielded a representative quantification of the confocal micrographs. The numbers and densities of CTB^+, $c\text{-}Fos^+$ and $CTB^+/c\text{-}Fos^+$ cells were determined, and the mean numbers/densities per hemisphere were calculated for each subject.

2.3.4 | Injection site validation

For validation of CTB-555 injection sites in NAc, images of complete coronal sections were acquired using a light epifluorescence microscope (Axio Observer. Z.1, Zeiss), 5× magnification, 0.55 NA and 26 mm WD, to visualize fluorescence.

2.4 | Establishing whether BA-NAc neurons are mono- or dual-valent with respect to social stimuli using TRAPing

The aim of this experiment was to focus on the AP BA region containing a high number of BA-NAc neurons responsive to SR and/or SA and investigate whether these neurons were mono- or dual-valent with respect to these social stimuli.

2.4.1 | Experimental design

Fos-TRAP2 mice ($n = 46$) were infused bilaterally in NAc with 300 nL of 1 mg/mL CTB-647 (Invitrogen). At 8–10 days post-surgery, mice were single-caged and, after a further 3–4 days, assigned at random to the following stimulus groups: social reward-social aversion (SR-SA, $n = 9$), SA-SR ($n = 8$; experimental social mice), SR-SR ($n = 8$), SA-SA ($n = 8$; control social mice), and no stimulus-no stimulus (No S-No S, $n = 11$). To adjust mice to the procedures of restraint and i.p. injection required for 4-hydroxytamoxifen (4-OHT) administration, on post-surgery Days 15–17 they received two daily i.p. injections of sterile 0.9% NaCl and one i.p. injection of castor oil:sunflower seed oil (1:4, 5 mL/kg). On Day 18, mice

underwent the first stimulus test, SR or SA (or No S), during t_{0-90}. Directly afterwards, they received an i.p. injection of 4-OHT. A period of 7 days was allowed for reporter recombination and expression; this was assumed to be sufficient based on in-house pilot tests and relevant literature (DeNardo et al., 2019; Guenthner et al., 2013). Mice then underwent the second stimulus exposure, SA or SR (or No S), during t_{0-90}. Directly afterwards, mice were deeply anaesthetized by injection of pentobarbital and transcardially perfused-fixed. The brains were further processed for c-Fos immunohistochemistry and quantification of CTB^+, $tdTomato^+$, $c\text{-}Fos^+$ neurons and combinations thereof, in the BA.

2.4.2 | 4-OHT preparation

4-OHT (Sigma, Cat# H6278) was dissolved completely at 20 mg/mL in 100% ethanol on a shaker at 37°C, which required about 15 min. The solution was then stored in 250 μL sealed aliquots at −20°C for up to several weeks. On the day of use, an aliquot of 4-OHT in ethanol was redissolved on a shaker at 37°C for about 15 min, and castor oil:sunflower seed oil mixture (1:4; Sigma, Cat #s 259853 and S5007) was added at a volume ratio of 1:2 (4-OHT: 6.7 mg/mL). The mixture was vortexed thoroughly for 1 min until the two phases were indistinguishable. The ethanol was then evaporated off via vacuum centrifugation to give a final concentration of 10 mg/mL 4-OHT. This was light protected and stored at 4°C until 30 min before injection, which occurred within 5–6 h of preparation. Based on in-house pilot tests and relevant literature, 4-OHT was injected i.p. at 50 mg/kg (DeNardo et al., 2019).

2.4.3 | Stimulus exposure protocols

All protocols were conducted between 9:00 AM and 1:00 PM. Social stimuli were presented as described for the BL/6 mouse experiment, except on the day prior to the first SR test, a female was introduced into the cage of the male until the first mount attempt, which took 2–15 min, and the female was then removed; this primed the male so that 'female' was not a novel stimulus in SR tests (Table S1). In experimental social mice (SR-SA and SA-SR), the order of exposure to SR and SA was counterbalanced, that is, nearly equal numbers of SR-SA and SA-SR mice were studied. In control social mice, the same stimulus type was presented twice, that is, SR-SR or SA-SA: in the case of SR, if the female that was SR at first exposure was not at (pro-)estrus on the day of second

exposure, then another female was used; in the case of SA, it was always the same CD-1 male in both tests. In the first experiment, based on the reasoning that males would not need prior experience of 'female' for females to be rewarding, no pre-exposure was used. Males did need to encounter ex-breeder CD-1 males to learn that such stimuli were aggressive and dominant, and hence, pre-exposure was used. One caveat of this approach was that there was a novelty difference between SR and SA. Therefore, in this experiment, there was a pre-exposure phase to both SR and SA testing. Comparing the findings of these experiments, the presence/absence of SR pre-exposure did not have a major impact on c-Fos activity in BA-NAc neurons.

2.4.4 | Immunohistochemistry and confocal microscopy

For c-Fos immunofluorescence, series of sections were collected from −1.6 to −2.0 mm, that is, the AP intermediate BA. Using the same custom-written Fiji macro as described for the BL/6 mouse experiment, the numbers and threshold grey values for CTB^+, $tdTom^+$, $c\text{-}Fos^+$, $CTB^+/tdTom^+$, $CTB^+/c\text{-}Fos^+$ and $CTB^+/tdTom^+/c\text{-}Fos^+$ cells/neurons were determined. The numbers and densities of cells/neurons were calculated as the sum of mean of both hemispheres per section for five sections (−1.6, −1.7, −1.8, −1.9 and −2.0). In addition, for c-Fos, the integrated density of each $c\text{-}Fos^+$ BA-NAc neuron was calculated as area × mean grey value.

The TRAPing parameters used were optimized by pilot study, in which reporter expression by BA cells (not specifically BA-NAc neurons) was quantified. A maximal efficacy of about 30% tdTom labelling of c-Fos labelling was realized, that is, if a stimulus (e.g. SR, SA and footshock) resulted in an average of 100 $c\text{-}Fos^+$ cells, it resulted in an average of 30 $tdTom^+$ cells. Protocol changes, including higher 4-OHT dose, signal amplification with tdTomato immunostaining, did not increase TRAPing efficacy.

2.5 | Assessing in vivo activity of intermediate BA-NAc neurons during SR using fibre photometry

The aim of this experiment was to focus on the AP BA region containing a high number of BA-NAc neurons responsive to SR and/or SA and to attempt to demonstrate engagement of these neurons during distal or proximal interactions with SR.

2.5.1 | Experimental design

BL/6 mice underwent stereotactic surgery required for conducting fibre photometry of GCaMP6-expressing BA-NAc neurons ($n = 12$) or, for purposes of controlling for signal artefacts, EGFP-expressing BA-NAc neurons ($n = 4$). Surgery was followed by a 21-day period of recovery and AAV vector expression. During the next 5 days, mice were habituated sequentially to: the testing room, being placed in the home cage in an attenuation chamber, being attached to the patch cord. Mice then underwent testing with an SR-fibre photometry protocol, conducted between 9:00 AM and 4:00 PM, that is, during the dark phase.

2.5.2 | Fibre photometry

Recombinant AAV vectors (Viral Vector Facility, Zurich Neuroscience Center, ETHZ/UZH) were used for pathway specific expression. For calcium-dependent fluorescent GCaMP6 expression in BA-NAc neurons, a vector encoding *GCaMP6* incorporated into a construct with FLEX, ssAAV-9/2-hSyn1-chI-dlox-GCaMP6m-dlox-WPRE-SV40p(A) (rAAV-FLEX-GCaMP6; 4.2×10^{12} vg/mL, 300 nL) (Grewe et al., 2017; Madur et al., 2023), was injected unilaterally in the BA (see Stereotactic surgery for retrograde tracing and fibre photometry). For Ca^{2+}-independent EGFP expression, as a control to determine whether certain social behaviours generated movement-related artefacts in the fibre photometry signal, a vector encoding *EGFP* incorporated into a construct with FLEX, ssAAV-9/2-hSyn1-dlox-EGFP (rev)-dlox-WPRE-hGHp(A) (rAAV-FLEX-EGFP; 8.2×10^{12} vg/mL, 300 nL; Grewe et al., 2017) was injected unilaterally in the BA. To induce *GCaMP6* or *EGFP* expression in BA-NAc neurons specifically, a retrograde vector encoding *Cre-recombinase*, rAAV-2-retro-hsyn1-Cre-mCherry (rAAV-retro-Cre; $8.4.10^{12}$ vg/mL, 300 nL) was injected in the ipsilateral NAc. After BA vector injection, a fibre-optic probe ($\varnothing = 200$ nm) was implanted directly above the injection site (bregma AP -1.8 mm, ML ± 3.2 mm, DV -4.9 mm). Stable adhesion of the fibre-optic probe onto the cranium was achieved as described previously (Ineichen et al., 2022; Madur et al., 2023). Mice were distributed equally in terms of whether the left or right hemisphere was studied.

Fibre photometry for optical recording of neural activity in freely moving mice was performed largely as described previously (Ineichen et al., 2022; Madur et al., 2023). Briefly, a laser as excitation light source, a high-sensitivity photoreceiver (model 2151, New Focus), and customized software for signal processing, were used. To provide excitation, a 488 nm laser light was focused

into a fibre patch cord and delivered at the optic fibre tip in the BA. The patch cord was connected via a ceramic sheath to the optic fibre ferrule on the mouse cranium. Back-propagated GCaMP6 or EGFP fluorescence was focussed on a photoreceiver, and custom-written software code was used for data acquisition (LABView Software, version 2020). Testing was conducted in an attenuation chamber equipped with a loudspeaker emitting low-level white noise. A camera (model C920, Logitech) was fixed to the underside of the ceiling of the attenuation chamber and allowed for video recording of the tests on the control PC running LabView. An opening in the ceiling of the attenuation chamber allowed for the passage of the patch cord. A modified cage lid was prepared out of transparent Plexiglas and contained an opening along its length to allow for passage of the patch cord and free movement of the mouse in the test cage during testing. Before the testing of each mouse, the cage lid and the divider used to divide the cage into two compartments were cleaned with 70% ethanol.

2.5.3 | Social reward-fibre photometry (SR-FP) protocol

Each SR-FP test comprised three consecutive phases of 20 min: no stimulus-FP to allow the mouse to adjust to the test environment including the patch cord and to check the optical signal, distal SR-FP and proximal SR-FP (Table S1). The mouse was transferred in its home cage to the attenuation chamber and connected to the patch cord for no stimulus-FP. It was then disconnected from the patch cord and transferred to the home cage of a (pro-)estrous female, which was separated longitudinally into two equal compartments by a transparent and perforated Plexiglas divider. The male and female were in separate compartments; the male was reconnected to the patch cord, and distal SR-FP was conducted during which the mice could have distal social contact, that is, approach and contact (Table S2). For proximal SR-FP, the divider was removed and the mice could have proximal socio-sexual contact (Table S2). The patch cord was then disconnected, and the mouse returned to its home cage. Two such tests were conducted on two consecutive days.

2.5.4 | Fibre photometry target validation

After completion of the experiment, mice were deeply anaesthetised and underwent brain perfusion-fixation for histological assessment in terms of BA probe placement and BA GCaMP6/EGFP and NAc mCherry expression.

As described in detail elsewhere (Ineichen et al., 2022; Madur et al., 2023), the optic fibre implant was removed, and the brain sectioned coronally at 100 μm using a vibratome (Leica). Sections underwent Nissl staining (NeuroTrace 640/660 Deep-Red Fluorescent Nissl Stain, Thermo Fisher), followed by washing in PBS, mounting on microscope slides, addition of Dako/DAPI fluorescence mounting medium (Sigma Aldrich) and cover-slipping. Using an epifluorescence microscope (Axio Observer.Z.1, Zeiss), mounting medium allowed for localization of GCaMP6/EGFP expression, and Nissl staining allowed for localization of the probe placement and tracing of the BA-NAc pathway using mCherry reporter. Using a mouse brain atlas (Franklin & Paxinos, 2019), the bregma levels of the BA section that included the most ventral position of the fibre tip in the BA and of the NAc section with the highest mCherry expression were identified. Two GCaMP6 mice were excluded due to a misplaced BA AAV vector injection and optic fibre placement, resulting in final sample sizes of $n = 10$ for GCaMP6 and $n = 4$ for EGFP.

2.5.5 | Analysis of SR-FP data

LABView files of video recording and of optical signal data were used to score social events using an ethogram (Table S2). Per test phase, the number and total duration of social episodes, and from this, the mean duration of each social episode, were calculated. The FP data for the first SR test were used for statistical analysis unless they included substantial artefacts in which case the second test was used (in the case of one mouse). Social events were manually time stamped onto the optical signal data. The time of each social event that resulted in the onset of a social episode, for example, approach, approach + mount, approach + copulation, was designated as t = 0 s. The fibre photometry data were analysed with custom-written MATLAB programmes (Ineichen et al., 2022; Madur et al., 2023). Optical signal data were demodulated at 970 Hz, down-sampled to a sampling frequency of 20 Hz and smoothed using an exponential smoothing function with damping factor 0.5, thereby excluding some of the broad-spectrum signal noise. The social event-specific mean Ca^{2+} (or EGFP) activity during the 5 s prior to event onset at t = 0 s provided the measure of baseline activity. For 10 s after social-event onset, regardless of the duration of the social episode that it initiated, for each 0.05 s time bin (t), the z-scored (normalized) signal intensity (F) was calculated using the formula $(F(t) − F_0)/SD_0$, where F_0 and SD_0 denote mean and standard deviation of 5-s baseline activity (mean z-scored Ca^{2+} baseline signal = 0). After the onset and

offset of a social episode, if the onset of the next social episode occurred within 10 s, this latter episode was not analysed; this was done in order to achieve some separation between baseline signal and social episode-related signal. For each mouse and each phase (distal SR, proximal SR), the mean peri-event/episode histogram was calculated, and these mouse-specific histograms were used to calculate the overall mean histograms per phase.

2.6 | Statistical analysis

Statistical analysis of immunohistochemical and fibre photometry data was conducted using GraphPad Prism (version 9.3). Data normality was assessed using the Shapiro–Wilk test and any outliers identified using Grubbs' test were excluded. For comparison of >2 means, homogeneity of variance was estimated via the Brown–Forsythe test and, if not met, Welch's ANOVA test was applied instead of ordinary one-way ANOVA. In two-way repeated measures ANOVA, sphericity was not assumed and Greenhouse–Geisser correction was applied. For the BL/6 experiment investigating the distribution of BA-NAc neurons responsive to SR and/or SA, data for neuronal number and density were analysed using two-way repeated measures ANOVAs, with a between-subjects factor of stimulus group (No S, SR and SA) and within-subjects factor of bregma level (from −1.0 to −2.6 mm). Significant interaction or main effects were analysed using Tukey's or Sidak's multiple comparison post hoc tests. For the TRAPing experiment investigating intermediate-BA-NAc neuron responsiveness to SR and/or SA, data for neuronal number were analysed using two-way repeated measures ANOVA, with a between-subjects factor of stimulus group (No S, SR-SA, SA-SR, SR-SR and SA-SA) and within-subjects factor of activity marker (tdTom and c-Fos). Significant interaction or main effects were analysed using Tukey's or Sidak's multiple comparison post hoc tests. Data for neuronal number are presented in the main text and for neuronal density in the Supporting Information, because neuronal number has been used in relevant publications this facilitates comparison (e.g. Beyeler et al., 2018; Kim et al., 2016). For the fibre photometry experiment, the z-scored Ca^{2+} (or EGFP) activity data in peri-event histograms were collapsed into one mean value for baseline and one mean value per 1 s time bin for the 10 s of post-event data, and a two-way repeated measures ANOVA was conducted with within-subjects factors of phase (distal and proximal) and time (from 0 to 10 s). The significant phase × time interaction effect was analysed between phases using Sidak's multiple comparison and, within phase, post-event Ca^{2+} activity at each 1 s time

bin was compared with baseline using Dunnett's multiple comparison test. Data are presented as mean ± SEM. Statistical significance was set at $p \leq .05$.

3 | RESULTS

3.1 | AP distributions of BA-NAc neurons activated by salient social stimuli

The first study aim was to determine the AP distribution profiles of BA neurons that project to NAc and are activated by salient social stimuli in terms of c-Fos protein expression (Figure 1a). C57BL/6J male mice were injected in the NAc core and shell at bregma +1.0–1.2 mm with the neuronal retrograde tracer, cholera toxin subunit β, conjugated with Alexa Fluor 555 (CTB-555; Figure S1a). After 10 days, mice were single-caged and after a further 3–4 days allocated randomly to stimulus groups (Figure 1b, Table S1). No S: the mouse remained undisturbed in the home cage to provide basal c-Fos levels for comparison. SR: a (pro-)estrous BL/6 female was placed into the home cage of the mouse for 90 min and distal and proximal socio-sexual interactions occurred; all SR mice approached, mounted and copulated with the female and penis licked (Table S2). SA: the mouse was placed in the home cage of an aggressive-dominant CD-1 male for 90 min, comprising periods of physical separation that allowed only distal social interactions, either side of a short period of proximal contact during which agonistic social interactions occurred without wounding, with all SA mice attacked for between 30 and 60 s during this proximal phase (Table S2). Following exposure to SR or SA (and No S), mice underwent brain perfusion-fixation. Brain coronal sectioning, c-Fos immunofluorescence staining, confocal microscopy and image quantification were conducted (Figure 1a,b).

In coronal sections that included the BA, immunostaining for neuronal and glial markers indicated that CTB was localized exclusively in glutamatergic neurons (Figure S2). In sections collected at 0.2 mm intervals from bregma −1.0 to −2.6, that is, the full AP extent of the BA, the absolute number of CTB+ BA-NAc neuronal cell bodies was maximal at −1.8 to −2.2 (consistent across groups), and they were distributed across the medial-lateral extent of the BA (bregma main effect: F[2.44, 85.44] = 109.10, p < .0001, Figure 1c; subregion main effect: F[1.41, 49.42] = 168.60, p < .0001, Figures 1f,i and S1b). A similar profile was observed using CTB+ BA-NAc neuron density (bregma main effect: F[1.7, 68.99] = 88.16, p < .0001; Figure S3a). It should be noted that when CTB-555 was injected more anteriorly in the NAc, namely, at +1.6, there was a corresponding anterior shift

in the distribution profile of CTB+ BA-NAc cell bodies (Figure S4); this indicates that BA-NAc neurons are organized topographically along the AP axis, demonstrating both the importance of the projection region targeted and the specificity of the current findings to the NAc region that we targeted.

In these same sections, the AP distribution profiles of total BA cells immunostained for c-Fos were determined: in both SR mice and SA mice, this number was substantially greater than in No S mice and maximal at −1.4 to −1.8. Whilst the AP profiles of BA c-Fos+ cells were overall rather similar in SR and SA mice, there were more such cells at −1.6 and −2.6 in SA than SR mice (stimulus group × bregma interaction effect: F[16, 280] = 7.71, p < .0001, Figure 1d; stimulus group × BA subregion interaction effect: F[4, 70] = 6.67, p = .0001, Figure 1g,i). Broadly, similar profiles were obtained using BA c-Fos+ cell density, except that the increase in SA versus SR mice was now specific to −2.6 (stimulus × bregma interaction effect (F[16, 280] = 4.44, p < .0001; Figure S3b). Anecdotally, in SR mice, most of the c-Fos+ neurons were in the medial BA with a minority in the lateral BA; for SA mice, the distribution was even more medially focused (Figure 1i); however, the medial-lateral distribution was not quantified. Focusing specifically on c-Fos+ neurons in the BA-NAc neuron pathway: in SR mice, the number was highest at −1.6 to −2.0 (int-BA), and SA mice had a similarly high number of c-Fos+ BA-NAc neurons at these same bregma levels. In SA mice specifically, this relatively high number of c-Fos+ neurons was also present at −2.4 to −2.6, such that SA mice had more c-Fos+ BA-NAc neurons than SR mice at these posterior bregma levels (stimulus group × bregma interaction effect: F[16, 280] = 6.52, p < .0001, Figure 1e; stimulus group × subregion interaction effect: F[4, 70] = 10.78, p < .0001, Figure 1h,i). Similar profiles were obtained using c-Fos+ BA-NAc neuron density (stimulus × bregma interaction effect: F[16, 280] = 5.14, p < .0001, Figure S3c). In terms of percentage of total CTB+ int-BA-NAc neurons, compared with 3.1% ± 0.5% in No S mice, 14.8% ± 2.1% were activated by SR and 17.2% ± 1.2% by SA; in post-BA-NAc neurons, the values were 2.4% ± 0.63%, 8.4% ± 0.8% and 13.1% ± 0.9%, respectively. To facilitate comparison with previous studies that have focussed on physical stimuli, another group of mice was exposed for 90 min to the fox odour-excrement constituent TMT (see e.g. Janitzky et al., 2015; Kim et al., 2016; Pérez-Gómez et al., 2015): compared with both SA and SR, fewer BA cells and fewer BA-NAc neurons were c-Fos+ in mice exposed to TMT (Figure S5).

Therefore, in terms of projectors to the NAc core/shell at bregma +1.0–1.2, it was not the case that the AP extent of the BA was divided into separate subregions that contained BA-NAc neurons responsive to either SR or to
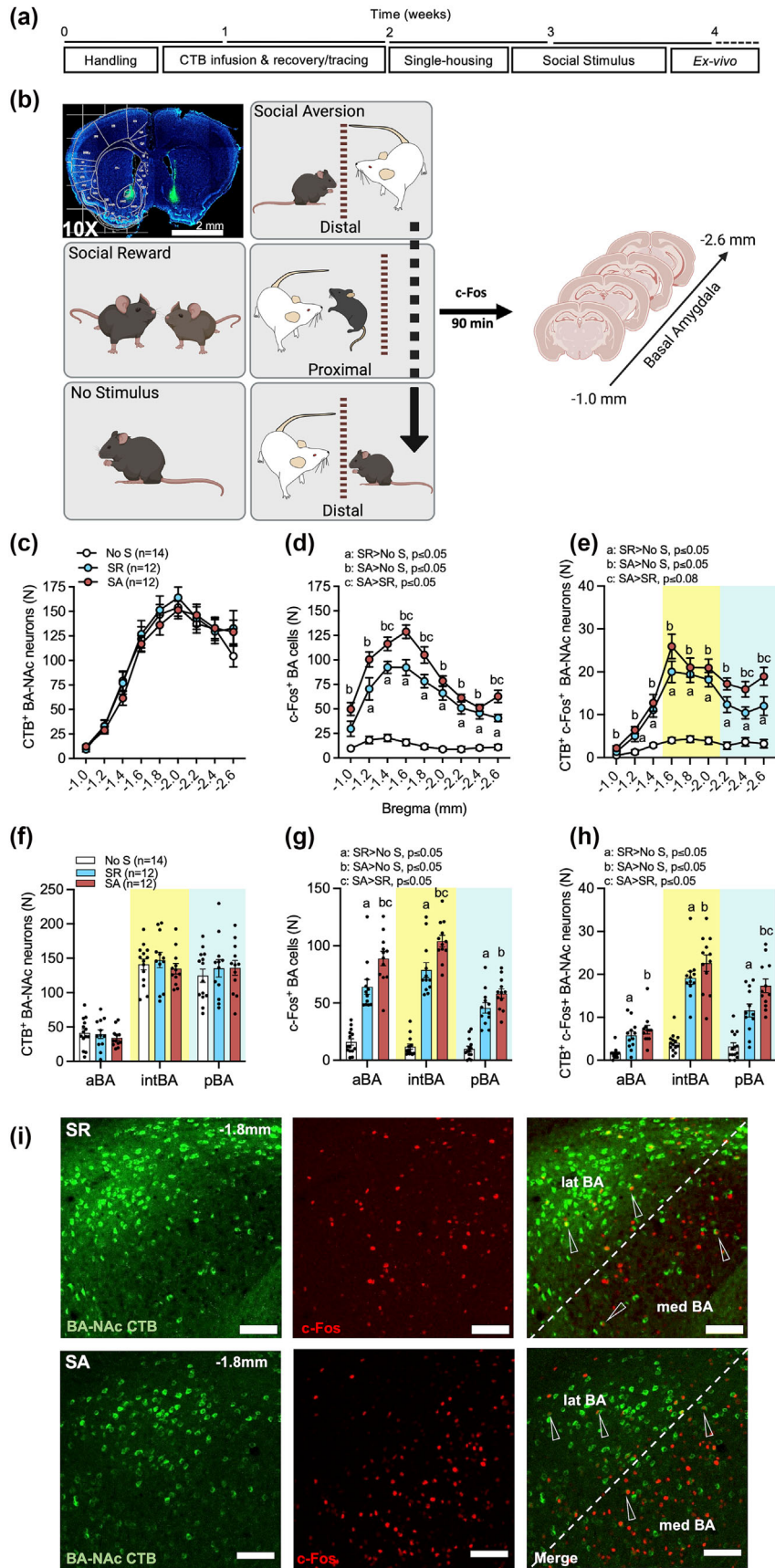
FIGURE 1 Legend on next page.

FIGURE 1 Anterior–posterior distribution of BA-NAc projection neurons and of their c-Fos activation by social reward (SR) or social aversion (SA). (a) Experimental design. Handling; CTB infusion & recovery/tracing: stereotactic surgery for bilateral CTB-Alexa Fluor 555 injection in NAc; single-housing; social stimulus: exposure to SR, SA or left undisturbed (no stimulus, No S); ex-vivo: 90 min after onset of SR or SA, social mice and No S were perfused-fixed. (b) Representative image (10x, scale bar = 2 mm) at bregma +1.1 showing NAc CTB injection. Schemas for stimulus exposures. (c–e): BA-NAc c-Fos expression, data are group mean $\pm$ SEM, with value for each mouse being the mean of both hemispheres for each bregma level. (c) Total CTB$^+$ BA-NAc neurons versus BA bregma level. Neuronal number depended on bregma level with highest number of neurons at -2.0. There was no main or interaction effect involving group ($p \geq .84$). (d) Total c-Fos$^+$ BA cells versus BA bregma level. SR and SA led to increased c-Fos$^+$ cells compared with No S mice, with highest number at -1.6; there were more c-Fos$^+$ cells in SA versus SR mice at -1.6 and -2.6. (e) CTB$^+$ c-Fos$^+$ BA-NAc neurons versus BA bregma level. SR and SA led to increased c-Fos$^+$ BA-NAc neurons compared with No S mice, with highest number at -1.6 to -2.0 (intermediate BA); there were more c-Fos$^+$ neurons in SA versus SR mice at -2.4 and -2.6 (posterior BA); different letters denote significant or trend-level pairwise post hoc stimulus-group differences using Tukey's multiple comparison. (f–h): the same data as in C-E now collapsed into BA subregions, anterior (aBA, -1.0 to -1.4), intermediate (int-BA, -1.6 to -2.0) and posterior (pBA, -2.2 to -2.6); data are individual values with mean $\pm$ SEM, with values for each mouse being the mean of both hemispheres $\times$ 3 bregma levels. (f) Total of CTB$^+$ BA-NAc neurons versus BA subregion. Neuronal number was similar in int-BA and pBA and higher than in aBA. There was no main or interaction effect involving group ($p \geq .67$). (g) Total c-Fos$^+$ BA cells versus BA subregion. In aBA and int-BA, SR and SA led to increased c-Fos$^+$ cells compared with no S mice, and SA led to increased c-Fos$^+$ cells compared with SR, whilst in pBA SR and SA led to a similar increase compared with No S. (h) CTB$^+$ c-Fos$^+$ BA-NAc neurons versus BA subregion. In aBA and int-BA, SR and SA led to a similar increase in c-Fos$^+$ BA-NAc neurons compared with No S, whilst in pBA SR and SA led to an increase in c-Fos$^+$ BA-NAc neurons compared with No S and SA to an increase compared with SR. (I) Representative confocal micrographs for left-hemisphere BA at bregma -1.8 from an SR mouse (upper images) and an SA mouse (lower images): left: CTB. Middle: c-Fos. Right: merged; the dashed line depicts the approximate medial and lateral subdivisions of the BA. Open arrows indicate examples of BA-NAc CTB$^+$/c-Fos$^+$ neurons. Scale bar = 100 μm. Brightness and contrast have been adjusted for display purposes.

SA. The int-BA had the highest number of NAc-projecting neurons activated by a (pro-)estrous female (SR), and this same region had a similarly high number of neurons activated by an aggressive-dominant male (SA). In the post-BA, more BA-NAc neurons were activated by SA than SR.

Whilst only indirectly relevant to the main aims of the study, the AP distributions of BA neurons responsive to SR or SA and projecting to medial-lateral compartments of the central amygdala (BA-CeA) were also investigated. The number of c-Fos$^+$ BA-CeA neurons was similar in SR and SA mice and rather consistent across the AP extent of the BA (Figure S6). These findings contrast with the somewhat surprising report that the vast majority of BA-CeA neurons are reward neurons (Kim et al., 2016).

3.2 | Evidence for monovalent intermediate BA-NAc neurons with respect to salient social stimuli

Having identified that in BL/6 mice the int-BA has a relatively high absolute number and density of NAc projectors that are engaged by salient social stimuli, in a next experiment the adult male offspring of Fos-TRAP2 x Ai14 mouse strains (DeNardo et al., 2019), referred to as Fos-TRAP2 mice, were studied to investigate whether these int-BA-NAc neurons are mono- or dual-valent with respect to SR and SA. TRAP allows for the study of

activation of an immediate early gene, in this case Fos, in the same neurons by two stimuli presented at different time points (Figure 2a). Whilst the efficacy of the TRAP-ing method is somewhat limited (Allen et al., 2017; Sanders et al., 2019), the literature indicates it to be adequate for current purposes given the inclusion of appropriate control groups.

Fos-TRAP2 male mice were injected in the NAc core/shell at bregma +1.0–1.2 mm with CTB-647 (Figures 2b and S7). After 10 days, mice were single caged and, after a further 3–4 days, underwent either No S, SR or SA, as described above (Figure 2c, Table S1). All mice were then injected with 4-OHT to induce Fos-dependent iCreER^{T2}-driven recombination, leading to permanent, cell-specific tdTom expression. After 7 days, mice in the experimental-social groups were exposed to the opposite social stimulus, SA or SR, for 90 min (i.e. SR-SA or SA-SR groups), mice in the control-social groups were re-exposed to the same social stimulus for 90 min (i.e. SR-SR or SA-SA groups), and No S mice remained No S (No S-No S group) (Figure 2c). All 25 SR mice (SR-SA, SA-SR and SR-SR) approached and mounted the female, and 17 of these copulated and penis licked, and in both exposures in the case of SR-SR mice (Table S2). All SA mice were attacked by the aggressive-dominant male for between 30 and 60 s during the proximate phase, and in both exposures in SA-SA mice (Table S2). All mice then underwent brain perfusion-fixation. Brains were sectioned coronally at int-BA -1.6 to -2.0, and c-Fos immunofluorescence staining,

confocal microscopy and image quantification were carried out.

As expected, the total number of CTB$^+$ int-BA-NAc neurons was similar across groups (Figure S8A). For total int-BA cells, the number of tdTom$^+$ int-BA cells was greater in mice exposed to SR or SA than in No S mice, and greater in mice exposed SA than in mice exposed to SR (main effect of stimulus group: F[4, 38] = 13.41, $p < .0001$; Figure S8b). In line with the limited efficacy of TRAPing, for each social-stimulus group, the total number of tdTom$^+$ int-BA cells was substantially less than that of c-Fos$^+$ int-BA cells (Figures 2g and S8b vs. c). The number of c-Fos$^+$ int-BA cells was highest in SA-SA mice (Welch's ANOVA, W[4.00, 17.96] = 162.8, $p < .0001$, Figure S8c).

Focusing on int-BA-NAc (CTB$^+$) neurons (Figure 2g), we first identified tdTom$^+$ neurons (Figure 2g), and then scored whether these were c-Fos$^-$ or c-Fos$^+$ (Figure 2g). The absolute number of tdTom$^+$ neurons was higher in each group of stimulus mice than in No S mice (stimulus group main effect: F[4, 39] = 6.01, $p = .0007$; a vs. b, $p < .05$, Figure 2d). In SR-SA and SA-SR mice, the absolute number of tdTom$^+$/c-Fos$^-$ neurons was higher than that of tdTom$^+$/c-Fos$^+$ neurons, whereas in control SR-SR and SA-SA mice these numbers were equable (stimulus group × activity marker interaction effect: F[4, 39] = 16.41, $p < .0001$, Figure 2d). This was confirmed by analysing the percentage of tdTom$^+$ neurons that were c-Fos$^+$ (group main effect: F[4, 39] = 39.01, $p < .0001$; Figure 2e): in mice exposed to SR-SA or SA-SR, 16.4% ± 2.1% (mean ± SEM, $n = 17$) of tdTom$^+$ neurons were also c-Fos$^+$, whereas in mice exposed to SR-SR or SA-SA, it was 49.8% ± 2.7% (mean ± SEM, $n = 16$). Given that about 50% of BA-NAc neurons were re-activated by re-exposure to SR or SA, then that only less than 20% of SR- or SA-activated BA-NAc neurons were re-activated by SA or SR, respectively, indicates that a substantial proportion of SR and SA responsive BA-NAc neurons are monovalent, at least with respect to these specific social stimuli. For tdTom$^-$ BA-NAc neurons (Figure 2f), more of these were c-Fos$^+$ in control-social (SR-SR and SA-SA) mice than in experimental-social (SR-SA and SA-SR) mice (W [4.00, 16.15] = 41.82, $p < .0001$), suggesting that first exposure to SR or SA leads to sensitization of the neuronal *c-Fos* response at re-exposure. Interestingly, this observed increase in the number of BA-NAc tdTom$^-$/c-Fos$^+$ neurons co-occurred with a reduced mean BA-NAc neuron c-Fos signal-intensity (group main effect: F [4, 39] = 17.68, $p < .0001$ Figure S9), consistent with a combination of sensitization of some and habituation of other neurons.

This experiment demonstrates that a substantial proportion of the intermediate BA neurons projecting to the NAc core/shell at bregma +1.0–1.2 are monovalent with respect to the social stimuli used, being engaged by either a (pro-)estrous female or an aggressive-dominant male, and with only a minority being engaged by both social stimuli. This finding was obtained despite the absolute number of social stimulus-responsive BA-NAc neurons likely being under-estimated due to the known quantitative limits of the TRAPing method.

3.3 | In vivo evidence for BA-NAc neuron population activity during interaction with SR

To complement the c-Fos-based ex vivo evidence that social stimuli engage intermediate BA-NAc neurons, in a third experiment, we investigated the in vivo activity of the int-BA-NAc neuron population during distal or proximal interactions with SR, using calcium-sensor fibre photometry (Figure 3a–c). For SA, a pilot study demonstrated that Ca^{2+} activity could not be recorded reliably during proximal exposure to an aggressive-dominant male due to risk of injury by (and damage to) the patch cord, and the experiment was therefore conducted with SR specifically. BL/6 male mice were injected in int-BA (−1.6/−2.0) with the AAV vector rAAV-FLEX-GCaMP6, or with rAAV-FLEX-EGFP in the case of signal-control mice, and in NAc core/shell (+1.0/1.3) with rAAV-retro-Cre, thereby achieving pathway-specific BA-NAc expression of intracellular calcium (Ca^{2+}) indicator GcaMP6 ($n = 10$) or of EGFP ($n = 4$). An optic fibre was positioned with its tip in the int-BA to enable GcaMP6- or EGFP-fluorescence detection (Figures 3c, S10). Whilst the SR stimulus was a (pro-)estrous female as in the c-Fos experiments, SR exposure was modified such that there were separate distal and proximal test phases (Table S1), allowing comparison of these two forms of sensory stimulation. Calcium (or EGFP) activity was recorded during a distal-SR phase (male separated from female via a perforated divider) and a proximal-SR phase (male and female with full contact). The SR tests were video recorded, and the onset and offset of social events/episodes (Table S2) were time stamped manually onto the fibre photometry signal trace.

For each measure, number of social events that initiated social episodes ($t(9) = 6.44$, $p < .0001$, Figure S11a), total duration of social episodes ($t(9) = 14.60$, $p < .0001$, Figure S11b) and the average duration of each social episode ($t(9) = 6.13$, $p < .0002$, Figure S11c), values were higher in the proximal-SR phase than in the distal-SR phase. The peri-event histograms for Ca^{2+} activity relative to onset of an episode of social behaviour are given in Figure 3d,e. In the distal-SR phase (Figure 3d), although social episodes were limited to the male facing the female on the opposite side of the divider, that is,
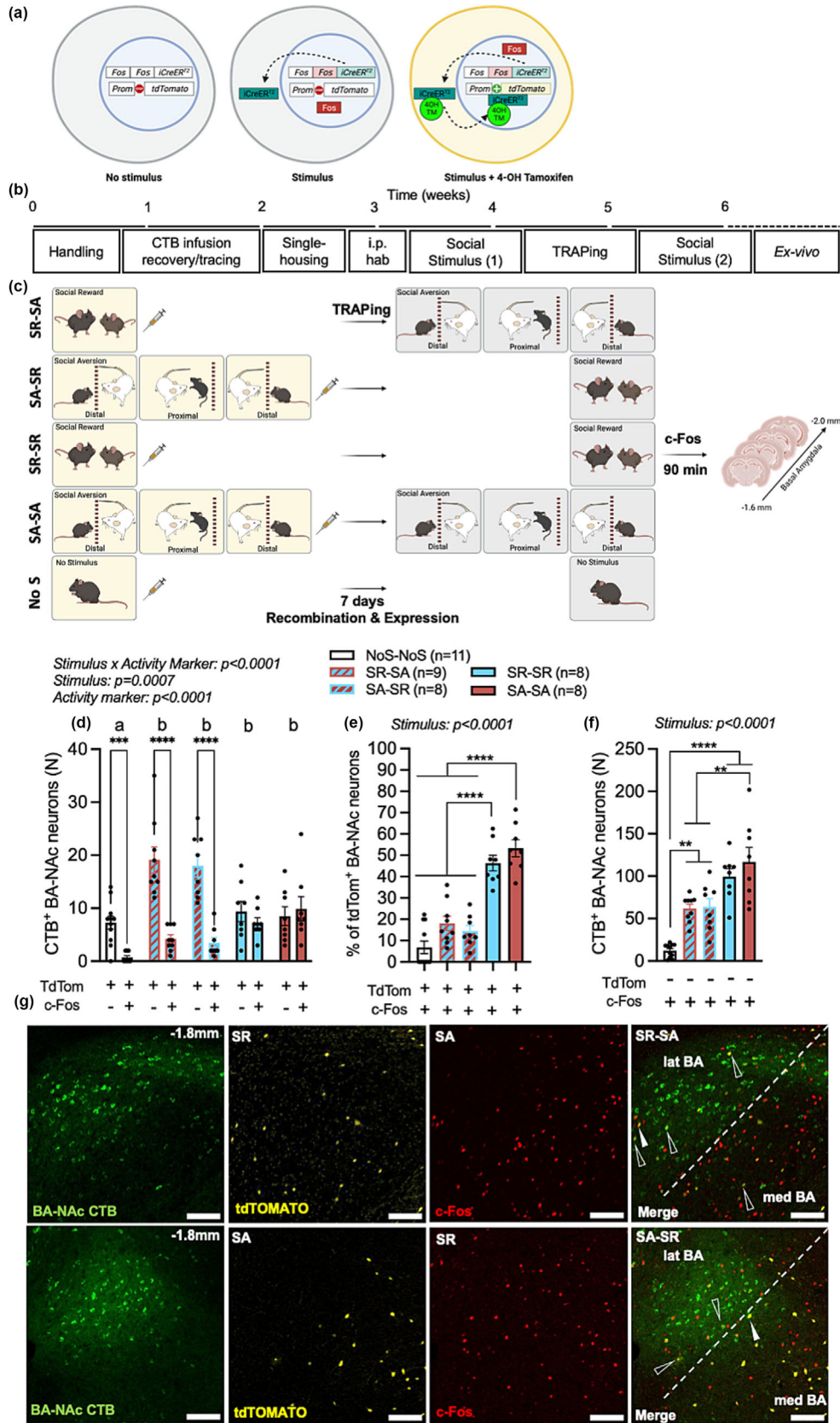
FIGURE 2 Legend on next page.

FIGURE 2 Activation of intermediate BA-NAc neurons by social reward and/or social aversion using TRAPing and c-Fos. (a) Schematic of TRAP system. In the presence of a salient stimulus, Fos promoter-Fos-iCreERT2 recombinase knock-in allele is activated/expressed. Endogenous c-Fos is expressed with a short half-life. iCreERT2 migrates to the cytosol, where it remains and degrades in the absence of 4-OHT. After 4-OHT injection, it binds to iCreERT2, the latter translocates to the nucleus, Cre-Lox recombination occurs at the tdTomato reporter knock-in allele, resulting in permanent expression of tdTomato. (b) Experimental design with Fos-TRAP2 male mice. (c) Schematic of experimental procedures. (d–f) tdTom and/or c-Fos expression by CTB^+ int-BA-NAc neurons: data are individual values calculated as the sum of [mean of both hemispheres per section] five sections (-1.6, -1.7, -1.8, -1.9 and -2.0), as well as group mean $\pm$ SEM. (d) Absolute number of $tdTom^+/c\text{-}Fos^-$ and $tdTom^+/c\text{-}Fos^+$ BA-NAc neurons. There were more activated ($tdTom^+$ and/or $c\text{-}Fos^+$) neurons in each of SR-SA, SA-SR, SR-SR and SA-SA mice than in No S mice. There were more $tdTom^+/c\text{-}Fos^-$ neurons than $tdTom^+/c\text{-}Fos^+$ in No S, SR-SA and SA-SR mice, and an equable number of such single- and double-labelled neurons in SR-SR and SA-SA mice. (e) Percentage of $tdTom^+$ BA-NAc neurons that were also $c\text{-}Fos^+$. Percentage was lower in experimental-social mice (SR-SA and SA-SR) and No S mice than in control-social mice (SR-SR and SA-SA). (f) Absolute number of $tdTom^-/c\text{-}Fos^+$ BA-NAc neurons. There were more such neurons in SR-SA and SA-SR mice than in No S mice, and there were more such neurons in SR-SR and SA-SA mice than in No S, SR-SA, SA-SR mice. Note the different Y-axis scales in D and F. (g) Representative confocal micrographs for left-hemisphere BA at bregma -1.8 from an SR-SA mouse (upper images) and an SA-SR mouse (lower images): left to right: CTB, tdTom, c-Fos, merged. in merged: open arrows indicate $CTB^+/tdTom^+/c\text{-}Fos^-$ (monovalent) BA-NAc neurons and filled arrows $CTB^+/tdTom^+/c\text{-}Fos^+$ (dual-valent) BA-NAc neurons. The merged images also indicate the approximate medial and lateral subdivisions of the BA. Scale bar $= 100$ μm. Brightness and contrast have been adjusted for display purposes.

distal contact, and had an average duration of 1–2 s, there was an increase in Ca^{2+} activity at seconds 3 and 4 after distal contact onset (phase $\times$ time interaction effect: F[2.31, 20.77] = 4.40, p = .02). In the proximal-SR phase (Figure 3e), social episodes comprised contact and sexual behaviours (Table S2): all 10 males mounted the female and 9 of 10 copulated and penis licked. There was an increase in Ca^{2+} activity at second 2 after the onset of proximal contact, and episodes had an average duration of 6–7 s (phase $\times$ time interaction effect: F[2.31, 20.77] = 4.40, p = .02). There was no time point at which there was a significant difference in post-event Ca^{2+} activity between the proximal-SR and distal-SR phases. Control mice expressed BA-NAc neuron EGFP, and this neuron activity-independent signal was applied to check for signal artefacts related to specific motor behaviours: EGFP mice had social interactions similar to those of GcaMP6 mice (Figure S11a–c); the peri-event mean EGFP signal remained relatively stable during the distal-SR (Figure S11d) and proximal-SR (Figure S11e) phases, indicating that the GcaMP6 signal changes were unlikely to have been motor-activity artefacts related to socio-sexual behaviours.

These in vivo social behaviour-related Ca^{2+} activity data complement the ex vivo data in demonstrating that int-BA-NAc neurons are indeed engaged by social stimuli; in this case, both distal and proximal interactions with a (pro-)estrous female.

4 | DISCUSSION

Conspecifics constitute emotionally salient stimuli. Furthermore, socio-sexual reward and aggressive-dominant aversion are largely independent of homeostatic states

such as hunger and thirst, rendering them more amenable to experimental study than the physical stimuli of food and water. In the present study of male mice, we demonstrate that: (1) the intermediate-to-posterior BA contains a relatively high number/density of glutamate neurons projecting to intermediate NAc core/shell. (2) Approximately 15% of int-BA-NAc neurons are activated by interaction with a (pro-)estrous female and 17% by interaction with an aggressive-dominant male, whereas for post-BA-NAc neurons it is 8% and 13%, respectively. Based on (1) and (2), the focus was placed on the int-BA to establish whether these neurons were mono- or dual-valent. (3) Using TRAPing, successive SR-SA or SA-SR exposure identified that the majority of int-BA-NAc neurons activated by SR are not activated by SA, and vice versa; that is, the majority of int-BA-NAc neurons are monovalent with respect to the social stimuli investigated. (4) Using GCaMP6 fibre photometry of an int-BA-NAc neuronal population, it could be demonstrated that these neurons are engaged during both distal and proximal interactions with SR. With respect to emotional stimuli in the social domain, and with caution required when extrapolating to non-social emotional stimuli, these findings advance current understanding of the organization of emotional stimulus processing by BA-NAc glutamate neurons in the mouse.

4.1 | New insights into the distribution of BA-NAc neurons activated by emotionally salient stimuli

The NAc core/shell bregma level of AP $+ 1.0$ to $+1.2$ was used in order to facilitate comparison with previous studies that investigated BA projections to NAc at $+1.0$ to
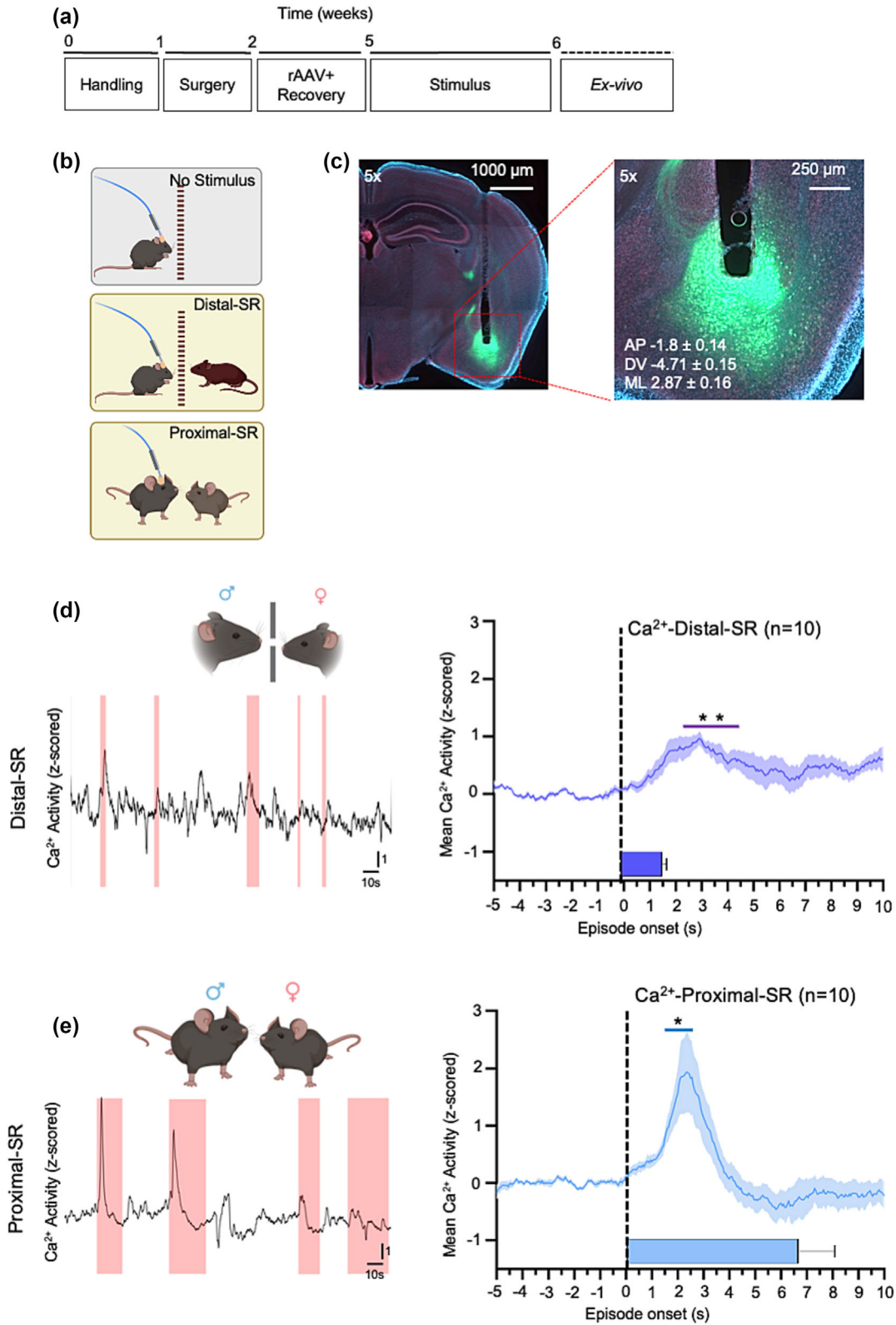
FIGURE 3 Legend on next page.

FIGURE 3 Assessment of intermediate BA-NAc neuron population activity during social reward-fibre photometry testing. (a) Experimental design. (b) Schematic of social reward-fibre photometry test phases: each session comprised the phases, each of 20 min, No stimulus, distal-SR, proximal-SR, with BA-NAc neuron activity ($n = 10$) or BA-NAc neuron EGFP signal ($n = 4$) recorded in each phase. For the phases, distal-SR and proximal-SR (yellow background), fibre photometry data were analysed in terms of Ca^{2+} activity (or EGFP signal) associated with social events. (c) Representative microscope image of a Nissl-stained coronal brain section showing location of the optic fibre implant including its tip in the BA at bregma -1.8 mm, and colocalized AAV vector-expressed GcaMP6 fluorescence. Right image: BA at high magnification with estimated coordinates of optic fibre tip placement (mean $\pm$ SD, $n = 10$). (d, e) Peri-event BA-NAc neuron Ca^{2+} activity during (d) distal-SR and (e) proximal-SR. Left: representative traces from individual mice showing 150 s of z-scored Ca^{2+} activity and concomitant social events, the latter depicted in pink shading. Right: Peri-event histograms of z-scored Ca^{2+} activity relative to social event onset (time = 0 s). The horizontal bars depict social event duration. Data are overall mean $\pm$ SEM values, $n = 10$ mice. There was a change in Ca^{2+} activity after the onset of social episodes during both distal-SR and proximal-SR, with activity increasing at seconds 3 and 4 in distal-SR and at second 2 in proximal-SR; there was no time point at which peri-event Ca^{2+} activity was significantly different between proximal and distal SR.

+1.5 (Kim et al., 2016; Namburi et al., 2015; Zhang et al., 2021). Retrograde tracer uptake by BA neuron somata was maximal at bregma -2.0 to -2.6 in terms of absolute number and density; this is similar to previous studies, which report a maximal number of BA-NAc neurons at -2.4 to -2.8 using percentage CTB^+ neurons/ large DAPI neurons (Kim et al., 2016) and at -2.0 using density (Beyeler et al., 2018). Moving the NAc injection site to $+1.6$ resulted in a corresponding, topographic shift in the AP distribution of BA-NAc neuron somata. The overall absolute number/density of BA-NAc neurons activated by social stimuli in terms of c-Fos was highest at BA -1.6 to -2.0 and comprised a similar amount of neurons responsive to SR and SA; at BA -2.6, there was a high absolute number/density of BA-NAc neurons activated by SA specifically. Relative to total BA-NAc neurons, in int-BA some 15%–17% were activated by SR or SA: this could reflect that 15%–17% of int-BA-NAc neurons are dual-valent 'social-stimulus' neurons, or that 30%–35% of int-BA-neurons are monovalent 'SR' or 'SA' neurons, or some combination of these two extremes. Using single BA-NAc neuron electrophysiological recording to identify neurons responsive to reward (sucrose) or aversion (quinine), 16% were excited by sucrose and only 3% by quinine, with 3% excited by both reward and aversion, and these neurons were distributed rather evenly along the AP axis of BA (Beyeler et al., 2016, 2018). Using single genes to distinguish between putative reward (female) neurons and putative aversion (foot shock) neurons, 70% and 30% of all BA-NAc neurons were purported to be reward and aversion neurons, respectively (Kim et al., 2016). Therefore, the current data indicate a relatively higher proportion of aversion-engaged BA-NAc neurons than was the case in previous studies. Related to this, we also assessed BA-NAc neuron activation by the physical aversive stimulus of TMT odour (Kim et al., 2016) and the number of activated neurons was substantially lower compared with social stimuli. This provides an indication of the relative salience of social

stimuli compared to a physical aversive stimulus; however, only one such stimulus was tested and no physical reward stimulus was investigated. Whilst the medial-lateral distribution of BA-NAc neurons responsive to SR and SA was not quantified, anecdotally, in the int-BA they were quite evenly distributed on the ML axis in both cases, consistent with their presence in both the medial anterior/magnocellular and lateral posterior/ parvocellular subregions (Pitkänen et al., 1997). This contrasts with the report that reward neurons are strictly parvocellular and aversion neurons magnocellular (Kim et al., 2016).

The retrograde tracer was injected into the NAc core primarily with some also being taken up by the shell directly ventral to the core. The NAc core and this subregion of the shell comprise primarily GABA-ergic medium spiny neurons (MSNs) expressing either dopamine receptor 1 (D1) or 2 (D2). The NAc core and shell are major regions of reward learning and motivation, and there is evidence that D1- and D2-MSNs contribute to this effect (Sesack & Grace, 2010). Investigation of the NAc shell along its anterior–posterior extent has demonstrated a gradient of subregions, or modules, involved in the regulation of appetitive (reward-approach) or defensive (aversion-avoidance) behaviour (Berridge, 2019). It is therefore possible that some SR- and SA-engaged BA-NAc neurons are projecting to appetitive and defensive subregions, respectively. Concerning the functionality of BA-NAc signalling, the small number of studies conducted to-date have focused on reward-directed behaviour. For example, excitation of BA neurons (not specifically BA-NAc neurons) facilitates dopamine-mediated reward-evoked firing by NAc neurons and subsequent reward-directed behaviour; that is, additive effects of BA glutamate neurons and dopamine neurons at NAc neurons (Ambroggi et al., 2008; Jones et al., 2010). In the BA-NAc neuronal pathway specifically, but without specific targeting of reward neurons, operant responding that triggered photo-stimulation of BA-NAc neurons was reinforcing as

—WILEY—

indicated by a reasonable level of intra-cranial self-stimulation (Namburi et al., 2015). In one study potentially specific to aversion processing, photo-stimulation of putative BA-NAc aversion neurons resulted in spontaneous defensive (freezing) behaviour (Kim et al., 2016). Beyond BA-NAc, the current findings also indicate the high number of BA cells activated by SR and/or SA that do not project to intermediate NAc core/shell: data for central amygdala are also included in this paper, and other projection regions are likely to include other AP-NAc subregions, as well as hippocampus and prefrontal cortex, among others (Beyeler et al., 2016, 2018; Burgos-Robles et al., 2017).

4.2 | Many intermediate BA-NAc neurons are monovalent with respect to SR and SA

Using physical reward and aversion stimuli, the evidence from single neuron recording is that most responsive intermediate BA-NAc neurons were engaged by one emotional valence specifically, with more neurons responding to reward than aversion (Beyeler et al., 2016, 2018; Namburi et al., 2015). Here, we used Fos-TRAP methodology combined with c-Fos immunostaining to investigate whether int-BA-NAc neurons that respond to SR also do so to SA, and vice versa. Relative to control-social mice in which about 50% of neurons that responded once to SR or to SA did so again at SR or SA re-exposure, a substantially lower proportion of BA-NAc neurons that responded to SR responded subsequently to SA, and vice versa. The number of neurons responding exclusively to SR or to SA was equable. Therefore, we conclude that the majority of int-BA-NAc neurons are monovalent with respect to SR and SA, and the number of neurons making up these two monovalent populations are similar. A previous study that used nicotine as reward and foot shock as aversion reported that the BA (not BA-NAc pathway specifically) contains intermingled populations of monovalent reward and aversion neurons, with activation also measured using c-Fos. Furthermore, *Fos*-dependent photo-stimulation of these neurons induced valence-specific and -relevant physiological and behavioural responses (Gore et al., 2015). The mice that we exposed twice to the same stimulus type provided essential control groups, and they also yielded important additional data on BA-NAc neuron engagement: firstly, more neurons were engaged by two exposures to SR or SA than were engaged by one exposure; second, the average intensity of neuronal c-Fos activation was lower at the second exposure. These findings are consistent with: weakly responsive (sub-threshold c-Fos activation) neurons

nonetheless forming a memory of the stimulus that sensitizes their activation at stimulus re-exposure; previously activated neurons forming a memory of the stimulus that habituates their activation at stimulus re-exposure.

4.3 | Intermediate BA-NAc neuronal population engagement during interactions with the social reward stimulus

Using bulk Ca^{2+}-activity fibre photometry, it was possible to measure the in vivo peri-event activity of int-BA-NAc neurons during distal or proximal interactions with SR. Evidence for engagement would constitute an important complement to the c-Fos based evidence that a substantial proportion of int-BA-NAc neurons are responsive to SR. Of course, there was the caveat that both putative SR- or SA-engaged sub-populations of monovalent neurons were recorded from, and it has been demonstrated that BA-NAc aversion neurons are inhibited by reward (Beyeler et al., 2016, 2018). Despite this, in both distal and proximal phases of the SR test, there were consistent and transient increases in BA-NAc neuron Ca^{2+} activity coincident with episodes of socio-sexual behaviour. In the distal-SR phase, the activity increase occurred at 3–4 s after social episode onset even though episodes were typically of 1–2 s duration, perhaps reflecting post-contact processing of sensory (e.g. olfactory) stimuli. In the proximal-SR phase, the activity increase occurred at 2 s after social episode onset, perhaps reflecting engagement during socio-sexual behavioural events including mounting and copulation (Kyriazi et al., 2018). Integrating the findings with those from electrophysiological studies of local field potentials, the extent to which groups of BA glutamate neurons fire in a synchronized manner during interactions with emotional stimuli is positively associated with gamma oscillations; such synchronicity might explain how relatively small populations of neurons, such as BA-NAc neurons, can make marked contributions to circuitries underlying the processing of emotional stimuli and related behaviour (Amir et al., 2018). Given the equivalence in the numbers of SA and SR BA-NAc neurons in the int-BA, it is parsimonious to assume that similar transient increases in activity would occur during the SA test.

5 | CONCLUSION

In conclusion, this study adds to the current understanding of BA-NAc neurons with respect to their organization for and engagement by stimuli of high emotional

salience. The intermediate BA with its magnocellular and parvocellular subregions contains a substantial number/density of NAc-projecting glutamate neurons that are monovalent with respect to estrous-receptive female and aggressive-dominant male. This novel, iterative ex vivo and in vivo evidence demonstrates the importance of this pathway in the circuitry of socio-emotional processing, and in particular, of studying the monovalent SR and SA BA-NAc neuronal sub-populations separately. This will need to include the study of causal involvement of these sub-populations in mouse models for psychopathologies of reward or aversion processing, that is, the psychopathologies that commonly occur in stress-related neuropsychiatric disorders.

AUTHOR CONTRIBUTIONS

Conceptualization: Giulia Poggi, Giorgio Bergamini, Redas Dulinskas, Bastian Hengerer and Christopher R. Pryce. *Methodology*: Giulia Poggi, Giorgio Bergamini, Redas Dulinskas, Alexandra Greter, Christian Ineichen and Hannes Sigrist. *Software*: Alexandra Greter and Christian Ineichen. *Validation*: Giulia Poggi, Giorgio Bergamini, Redas Dulinskas, Alexandra Greter and Christian Ineichen. *Formal analysis*: Giulia Poggi, Redas Dulinskas and Alexandra Greter. *Investigation*: Giulia Poggi, Giorgio Bergamini, Redas Dulinskas, Lorraine Madur, Alexandra Greter, Christian Ineichen, Amael Dagostino, Diana Kúkeľová and Hannes Sigrist. *Resources*: Christopher R. Pryce. *Data curation*: Christopher R. Pryce. *Writing—original draft*: Giulia Poggi, Redas Dulinskas, Lorraine Madur and Christopher R. Pryce. *Writing—review and editing*: Giulia Poggi, Giorgio Bergamini, Redas Dulinskas, Lorraine Madur, Alexandra Greter, Christian Ineichen, MB, Amael Dagostino, Diana Kúkeľová, Hannes Sigrist, Klaus D. Bornemann, Bastian Hengerer and Christopher R. Pryce. *Visualization*: Giulia Poggi, Redas Dulinskas and Lorraine Madur. *Supervision*: Christopher R. Pryce. *Project administration*: Giulia Poggi, Klaus D. Bornemann and Christopher R. Pryce. *Funding acquisition*: Christopher R. Pryce.

ACKNOWLEDGEMENTS

CONFLICT OF INTEREST STATEMENT

K.D. Bornemann and Bastian Hengerer are employees of Boehringer Ingelheim Pharma AG.

PEER REVIEW

The peer review history for this article is available at https://www.webofscience.com/api/gateway/wos/peer-review/10.1111/ejn.16272.

DATA AVAILABILITY STATEMENT

Data are available upon request.

ORCID

Christopher R. Pryce https://orcid.org/0000-0002-5614-4690

REFERENCES

Allen, W. E., Denardo, L. A., Chen, M. Z., Liu, C. D., Loh, K. M., Fenno, L. E., Ramakrishnan, C., Deisseroth, K., & Luo, L. (2017). Thirst-associated preoptic neurons encode an aversive motivational drive. *Science*, *357*, 1149–1155. https://doi.org/10.1126/science.aan6747

Ambroggi, F., Ishikawa, A., Fields, H. L., & Nicola, S. M. (2008). Basolateral amygdala neurons facilitate reward-seeking behavior by exciting nucleus Accumbens neurons. *Neuron*, *59*, 648–661. https://doi.org/10.1016/j.neuron.2008.07.004

Amir, A., Headley, D. B., Lee, S. C., Haufler, D., & Paré, D. (2018). Vigilance-associated gamma oscillations coordinate the ensemble activity of basolateral amygdala neurons. *Neuron*, *97*, 656–669.e7. https://doi.org/10.1016/j.neuron.2017.12.035

Baxter, M. G., & Murray, E. A. (2002). The amygdala and reward. *Nature Reviews. Neuroscience*, *3*, 563–573. https://doi.org/10.1038/nrn875

Belova, M. A., Paton, J. J., Morrison, S. E., & Salzman, C. D. (2007). Expectation modulates neural responses to pleasant and aversive stimuli in primate amygdala. *Neuron*, *55*, 970–984. https://doi.org/10.1016/j.neuron.2007.08.004

Berridge, K. C. (2019). Affective valence in the brain: Modules or modes? *Nature Reviews. Neuroscience*, *20*, 225–234. https://doi.org/10.1038/s41583-019-0122-8

Beyeler, A., Chang, C.-J., Silvestre, M., Lévêque, C., Namburi, P., Wildes, C. P., & Tye, K. M. (2018). Organization of Valence-Encoding and Projection-Defined Neurons in the basolateral amygdala. *Cell Reports*, *22*, 905–918. https://doi.org/10.1016/j.celrep.2017.12.097

Beyeler, A., Namburi, P., Glober, G. F., Simonnet, C., Calhoon, G. G., Conyers, G. F., Luck, R., Wildes, C. P., & Tye, K. M. (2016). Divergent routing of positive and negative information from the amygdala during memory retrieval. *Neuron*, *90*, 348–361. https://doi.org/10.1016/j.neuron.2016.03.004

Burgos-Robles, A., Kimchi, E. Y., Izadmehr, E. M., Porzenheim, M. J., Ramos-Guasp, W. A., Nieh, E. H., Felix-Ortiz, A. C., Namburi, P., Leppla, C. A., Presbrey, K. N., Anandalingam, K. K., Pagan-Rivera, P. A., Anahtar, M., Beyeler, A., & Tye, K. M. (2017). Amygdala inputs to prefrontal cortex guide behavior amid conflicting cues of reward and punishment. *Nature Neuroscience*, *20*, 824–835. https://doi.org/10.1038/nn.4553

DeNardo, L. A., Liu, C. D., Allen, W. E., Adams, E. L., Friedmann, D., Fu, L., Guenthner, C. J., Tessier-Lavigne, M., & Luo, L. (2019). Temporal evolution of cortical ensembles promoting remote memory retrieval. *Nature Neuroscience*, *22*, 460–469. https://doi.org/10.1038/s41593-018-0318-7

Duvarci, S., & Pare, D. (2014). Amygdala microcircuits controlling learned fear. *Neuron*, *82*, 966–980. https://doi.org/10.1016/j.neuron.2014.04.042

Ekambaram, G., Sampath Kumar, S. K., & Joseph, L. D. (2017). Comparative study on the estimation of estrous cycle in mice by visual and vaginal lavage method. *Journal of Clinical and Diagnostic Research*, *11*, AC05–AC07. https://doi.org/10.7860/JCDR/2017/23977.9148

Franklin, K., & Paxinos, G. (2019). *The mouse brain in stereotaxic coordinates* (V. ed.). Elsevier.

Gore, F., Schwartz, E. C., Brangers, B. C., Aladi, S., Stujenske, J. M., Likhtik, E., Russo, M. J., Gordon, J. A., Salzman, C. D., & Axel, R. (2015). Neural representations of unconditioned stimuli in basolateral amygdala mediate innate and learned responses. *Cell*, *162*, 134–145. https://doi.org/10.1016/j.cell.2015.06.027

Grewe, B. F., Gründemann, J., Kitch, L. J., Lecoq, J. A., Parker, J. G., Marshall, J. D., Larkin, M. C., Jercog, P. E., Grenier, F., Li, J. Z., Lüthi, A., & Schnitzer, M. J. (2017). Neural ensemble dynamics underlying a long-term associative memory. *Nature*, *543*, 670–675. https://doi.org/10.1038/nature21682

Griffin, J. M., Fuhrer, R., Stansfeld, S. A., & Marmot, M. (2002). The importance of low control at work and home on depression and anxiety: Do these effects vary by gender and social class? *Social Science & Medicine*, *54*, 783–798. https://doi.org/10.1016/S0277-9536(01)00109-5

Guenthner, C. J., Miyamichi, K., Yang, H. H., Heller, H. C., & Luo, L. (2013). Permanent genetic access to transiently active neurons via TRAP: Targeted recombination in active populations. *Neuron*, *78*, 773–784. https://doi.org/10.1016/j.neuron.2013.03.025

Gururajan, A., Reif, A., Cryan, J. F., & Slattery, D. A. (2019). The future of rodent models in depression research. *Nature Reviews. Neuroscience*, *20*, 686–701. https://doi.org/10.1038/s41583-019-0221-6

Ineichen, C., Greter, A., Baer, M., Sigrist, H., Sautter, E., Sych, Y., Helmchen, F., & Pryce, C. R. (2022). Basomedial amygdala activity in mice reflects specific and general aversion uncontrollability. *European Journal of Neuroscience*, *55*, 2435–2454. https://doi.org/10.1111/ejn.15090

Janitzky, K., D'Hanis, W., Kröber, A., & Schwegler, H. (2015). TMT predator odor activated neural circuit in C57BL/6J mice indicates TMT-stress as a suitable model for uncontrollable intense stress. *Brain Research*, *1599*, 1–8. https://doi.org/10.1016/j.brainres.2014.12.030

Johansen, J. P., Cain, C. K., Ostroff, L. E., & Ledoux, J. E. (2011). Molecular mechanisms of fear learning and memory. *Cell*, *147*, 509–524. https://doi.org/10.1016/j.cell.2011.10.009

Jones, J. L., Day, J. J., Aragona, B. J., Wheeler, R. A., Wightman, R. M., & Carelli, R. M. (2010). Basolateral amygdala modulates terminal dopamine release in the nucleus Accumbens and conditioned responding. *Biological Psychiatry*, *67*, 737–744. https://doi.org/10.1016/j.biopsych.2009.11.006

Kim, J., Pignatelli, M., Xu, S., Itohara, S., & Tonegawa, S. (2016). Antagonistic negative and positive neurons of the basolateral amygdala. *Nature Neuroscience*, *19*, 1636–1646. https://doi.org/10.1038/nn.4414

Kirschbaum, C., Pirke, K.-M., & Hellhammer, D. H. (2004). The 'Trier social stress test' – A tool for investigating psychobiological stress responses in a laboratory setting. *Neuropsychobiology*, *28*, 76–81. https://doi.org/10.1159/000119004

Kyriazi, P., Headley, D. B., & Pare, D. (2018). Multi-dimensional coding by basolateral amygdala neurons. *Neuron*, *99*, 1315–1328.e5. https://doi.org/10.1016/j.neuron.2018.07.036

Lüthi, A., & Lüscher, C. (2014). Pathological circuit function underlying addiction and anxiety disorders. *Nature Neuroscience*, *17*, 1635–1643. https://doi.org/10.1038/nn.3849

Madisen, L., Zwingman, T. A., Sunkin, S. M., Oh, S. W., Zariwala, H. A., Gu, H., Ng, L. L., Palmiter, R. D., Hawrylycz, M. J., Jones, A. R., Lein, E. S., & Zeng, H. (2010). A robust and high-throughput Cre reporting and characterization system for the whole mouse brain. *Nature Neuroscience*, *13*, 133–140. https://doi.org/10.1038/nn.2467

Madur, L., Ineichen, C., Bergamini, G., Greter, A., Poggi, G., Cuomo-Haymour, N., Sigrist, H., Sych, Y., Paterna, J.-C., Bornemann, K. D., Viollet, C., Fernandez-Albert, F., Alanis-Lobato, G., Hengerer, B., & Pryce, C. R. (2023). Stress deficits in reward behaviour are associated with and replicated by dysregulated amygdala-nucleus accumbens pathway function in mice. *Communications Biology*, *6*, 422. https://doi.org/10.1038/s42003-023-04811-4

McEwen, B. S. (2007). Physiology and neurobiology of stress and adaptation: Central role of the brain. *Physiological Reviews*, *87*, 873–904. https://doi.org/10.1152/physrev.00041.2006

Namburi, P., Beyeler, A., Yorozu, S., Calhoon, G. G., Halbert, S. A., Wichmann, R., Holden, S. S., Mertens, K. L., Anahtar, M., Felix-Ortiz, A. C., Wickersham, I. R., Gray, J. M., & Tye, K. M. (2015). A circuit mechanism for differentiating positive and negative associations. *Nature*, *520*, 675–678. https://doi.org/10.1038/nature14366

Pérez-Gómez, A., Bleymehl, K., Stein, B., Pyrski, M., Birnbaumer, L., Munger, S. D., Leinders-Zufall, T., Zufall, F., & Chamero, P. (2015). Innate predator odor aversion driven by parallel olfactory subsystems that converge in the ventromedial hypothalamus. *Current Biology*, *25*, 1340–1346. https://doi.org/10.1016/j.cub.2015.03.026

Pitkänen, A., Savander, V., & LeDoux, J. E. (1997). Organization of intra-amygdaloid circuitries in the rat: An emerging framework for understanding functions of the amygdala. *Trends in Neurosciences*, *20*, 517–523. https://doi.org/10.1016/S0166-2236(97)01125-9

Pryce, C. R., & Fuchs, E. (2017). Chronic psychosocial stressors in adulthood: Studies in mice, rats and tree shrews. *Neurobiol Stress*, *6*, 94–103. https://doi.org/10.1016/j.ynstr.2016.10.001

Rosen, J. B., Asok, A., & Chakraborty, T. (2015). The smell of fear: Innate threat of 2,5-dihydro-2,4,5-trimethylthiazoline, a single molecule component of a predator odor. *Frontiers in Neuroscience*, *9*, 292. https://doi.org/10.3389/fnins.2015.00292

Sanders, K. M., Sakai, K., Henry, T. D., Hashimoto, T., & Akiyama, T. (2019). A subpopulation of amygdala neurons mediates the affective component of itch. *Journal of Neuroscience*, *39*, 3345–3356. https://doi.org/10.1523/JNEUROSCI.2759-18.2019

Schindelin, J., Arganda-Carreras, I., Frise, E., Kaynig, V., Longair, M., Pietzsch, T., Preibisch, S., Rueden, C., Saalfeld, S., Schmid, B., Tinevez, J. Y., White, D. J., Hartenstein, V., Eliceiri, K., Tomancak, P., & Cardona, A. (2012). Fiji: An open-source platform for biological-image analysis. *Nature Methods*, *9*, 676–682. https://doi.org/10.1038/nmeth.2019

Sesack, S. R., & Grace, A. A. (2010). Cortico-basal ganglia reward network: Microcircuitry. *Neuropsychopharmacology*, *35*, 27–47. https://doi.org/10.1038/npp.2009.93

Zhang, X., Guan, W., Yang, T., Furlan, A., Xiao, X., Yu, K., An, X., Galbavy, W., Ramakrishnan, C., Deisseroth, K., Ritola, K., Hantman, A., He, M., Josh Huang, Z., & Li, B. (2021). Genetically identified amygdala–striatal circuits for valence-specific behaviors. *Nature Neuroscience*, *24*, 1586–1600. https://doi.org/10.1038/s41593-021-00927-0

SUPPORTING INFORMATION

Additional supporting information can be found online in the Supporting Information section at the end of this article.